GENES4/ANP2003, Sep. 15-19, 2003, Kyoto, JAPAN
Paper 1112

Prediction of Multi-Dimensional Void Fraction Distribution in Upward Bubbly Two-Phase Flow with Sudden Expansion

Koichi KONDO*, Kenji YOSHIDA, Tomio OKAWA, Tadayoshi MATSUMOTO and Isao KATAOKA
[1]*Department of Marine Engineering, Marine Technical College, Ashiya, 659-0026, Japan*
[2]*Department of Mechanophysics Engineering, Osaka University, Osaka 565-0871, Japan*

Experimental and analytical studies were made on the multi-dimensional behavior of upward gas-liquid two-phase flow in a vertical pipe with an axisymmetric sudden expansion, which is one of the typical multi-dimensional channel geometries. The first, the local void fractions in the tube cross sections were measured at several downstream positions of the sudden expansion using a point-electrode resistivity probe for various gas and liquid flow conditions. The second, Lagrangian simulation of a single bubble behavior in the turbulent flow field, in which the motion of each bubble is individually tracked using a 3D one-way bubble tracking method which takes into account shear-induced and wall-induced lift forces, drag force, virtual mass force and buoyant force, was carried out. Based on the trajectories of large number of bubbles, the void fraction distributions were predicted for the sudden expansion channel. In this report, both experimental and numerical results were compared with the bubble diameter and the flow rates of gas and liquid phase. As a result, it was demonstrated that the single bubble distribution in the sudden pipe expansion was made a rough estimate by the present model. It also pointed out for accurate prediction that lift force, two-phase turbulence model, bubble interaction, coalescence, breakup and stagnation of bubbles occurred by the sudden expansion would be important factors in determining lateral void fraction distribution.

KEYWORDS: sudden expansion, void fraction distribution, single bubble, bubble tracking method

I. Introduction

Multi-dimensional behavior of gas-liquid two-phase flow is quite important in accurately evaluating safety and performance of nuclear reactor. In recent years, much research efforts have been devoted to the modeling, prediction and experiment on this phenomenon. However, even in the simplest system such as pipe flow, the established method has not been developed yet.

In our previous studies[1, 2], experimental and analytical approaches were made on the multi-dimensional behavior of upward gas-liquid two-phase flow through a vertical pipe with an axisymmetric sudden expansion, which is one of the typical multi-dimensional channel geometries. Phenomena in the sudden expansion have been experimentally revealed; the flow regime map and the flow patterns at the below and above of the sudden expansion point were classified with the bubble diameter. The direct observation using high-speed video camera captured the characteristic phenomena of bubbles and gas-slug caused by the sudden expansion. The void fraction distributions along the flow direction at the below and above of the sudden expansion were measured for various flow conditions. These results showed that quite complicated behaviors depending upon flow rates of gas and liquid phases. In particular, in the geometry of sudden expansion, very high shear rate region and backward flow region appear and these flow fields have complicated effects on the bubble behaviors in multi-dimensional two-phase flow.

* Corresponding author, Tel.+81-797-38-6292, Fax.+81-797-32-5972, E-mail: kondou@mail.mtc.ac.jp

In practical applications, however, multi-dimensional analyses cannot be always carried out and the prediction for behavior of two-phase flow in multi-dimensional channel is also important. A two-fluid model is commonly used for the prediction of averaged two-phase flow behavior[3-5]. Since constitutive equations of two-fluid model are developed based on the experimental data under steady state of developed two-phase flow in a pipe, it is quite important to evaluate the applicability of two-fluid model and its constitutive equations to the multi-dimensional two-phase flow analysis. We have confirmed the applicability of two-fluid model to one-dimensional two-phase flow analysis in the sudden expansion. The cross-sectional averaged void fractions along the flow direction were calculated by using the one-dimensional two-fluid model considering the phase distribution parameter to confirm the applicability of the computations[6]. From the calculation, the two-phase flow behavior even in the sudden expansion might be predicted to a certain extent using the one-dimensional two-fluid model. Simultaneously, it concretely pointed out that some multi-dimensional modeling or modifications for numerical simulation would be needed for more accurate prediction of two-phase flow.

The two-fluid model has difficulties for taking into account the bubble size distribution, bubble coalescence and breakup in bubbly flow calculation. In addition, excessive numerical diffusion arises due to the fully averaged nature of the model. In order to estimate appropriate accuracy the multi-dimensional behavior of two-phase flow, several more detailed two-phase flow models have been proposed. A bubble tracking method is one of these promising models.

In this method, an Eulerian description is used for the continuous liquid phase as in the case of the two-fluid model, while the motion of each bubble is individually tracked using a Lagrangian description[7-9].

In view of these, measurements and predictions were carried out on multi-dimensional void fraction distributions in the present study. The first, the local void fractions in the tube cross sections were measured at several downstream positions of the sudden expansion using a point-electrode resistivity probe for various gas and liquid flow conditions. The results of detailed void fraction measurements showed that how the two-phase flow develops along the flow direction of the downstream of the sudden expansion. Next, the motion of single bubbles in the turbulent flow field in sudden expansion channel was calculated using a three dimensional one-way bubble tracking method, in which it takes into account shear-induced and wall-induced lift forces, drag force, virtual mass force, buoyancy and wall shear forces. As the first step of the calculation, the velocity data of liquid single-phase flow calculated by standard k-ε model was used for this calculation. Based on the trajectories of large number of bubbles, the void fraction distributions were predicted. Both experimental and numerical results were compared with the bubble diameter and the flow rates of gas and liquid phase in the sudden expansion. The effects of bubble size, flow rates of gas and liquid phase, lift force acting on bubble etc. would be evaluated by using the bubble tracking method. Through these results, some discussions will be made on a question whether the phase distribution can be predicted by the bubble tracking method in a multi-dimensional pipe or not.

II. Experiment

1.Experimental Setup

A schematic diagram of the experimental apparatus is shown in **Fig. 1**. In this experiment, a vertical, upward, air-water two-phase flow at near atmospheric conditions was formed in an optically clear pipe with an axisymmetric sudden expansion, which consists of 20-mm tube and 50-mm tube. The vertical section of test channel (11) is approximately 6.0 m in length; the upstream of sudden expansion is a 2.4 m long and 20 mm in diameter of entrance section, and the downstream of sudden expansion is a 3.5 m long and 50 mm in diameter.

The centrifugal pump (3) discharge the water out from the storage tank (2), it reaches to bubble generator (10) passing through flow control valve (4), flow rotameter (5). After passing the test channel (11), the air or bubbles are removed at air-water separator (12), after that the water flows back to storage tank. The water cooler (13) keeps the water temperature constant during the experiment. The air is pressurized using the air compressor (6), and it is accumulated into the pressurized air tank (7) after drying up with the air-dryer. The compressed air in the pressurized tank is introduced to the bubble generator passing through the flow control regulator (8) and the flow rotameter (9). The air is injected into the test channel using the bubble generator. In this case, the bubble generator was installed at the center of the tube, and it consists of a sintered stainless steel block, 10 mm in diameter and 38 mm in height, having a particle-passing diameter of 1.0 μm.

In the sudden expansion channel, the volumetric flux of gas phase was employed as that of the below of the sudden expansion because it was difficult to identify the value of the pressure in the such geometry. Therefore, the volumetric flux of gas and liquid phases in 20-mm tube were used as parameters for the flow conditions of the sudden expansion. For the experiment, the volumetric fluxes of both phases or the water and the air superficial velocities in 20-mm tube were set to be at j_{L20} = 0-5.31 [m/s], j_{G20} = 0.05-0.6 [m/s], respectively.

2.Void Fraction Measurement

Figure 2 and **3** show the void fraction measurement system. The resistivity probe design is schematically shown in **Fig. 2**. It is a straight type probe, or so-called I-type probe. The I-type probe was employed in this experiment, because the multi-dimensional behaviors appear in sudden expansion channel. A wire of the point-electrode probe is made of stainless steel wire with a diameter of 0.2 mm. The wire is inserted into Teflon-insulated tube of 0.36 mm in diameter. The tip of the wire is coated with insulating enamel, and it is dried up to ensure a well insulation at 200

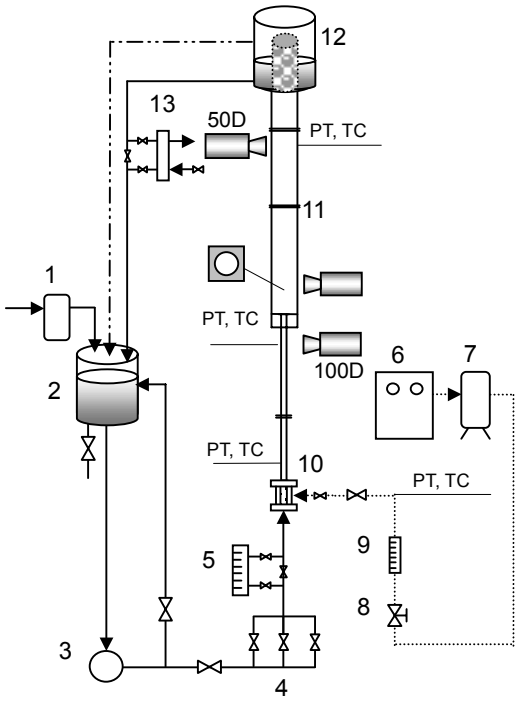

1. Filter (5 μm)
2. Storage tank
3. Water pump
4. Water flow control valve
5. Water flow meter
6. Air compressor & Dryer
7. Pressurized air tank
8. Air flow Regulator
9. Air flow meter
10. Bubble generator
11. Test channel
12. Air-water separator
13. Water cooler

Fig. 1 Experimental apparatus

degree centigrade. Furthermore, this wire is inserted into another stainless steel tube, 2.0 mm in diameter. The electric signal from the probe is come in to the PC using the void-signal processing. The void fraction data was detected by sampling frequency of 10 kHz and sampling time of 60 seconds. The test channel for the local void fraction measurement is shown in **Fig. 3** and it can be traversed the radial and axial position. Therefore the local void fraction distributions across the tube cross-sections of the sudden expansion are measured by changing the axial positions.

As the volumetric extension of gas phase due to the variation of static pressure had to be taken into account in the downstream position along the flow direction, the volumetric flux of gas phase at the measurement points were corrected by using the pressure and temperature of liquid phase measured by the pressure transducer (PT) and thermo couple (TC). In void fraction measurements, the pressure and the temperature measured of liquid phase at each measurement point were employed to correct the volumetric flux of gas phase (see **Fig. 3**).

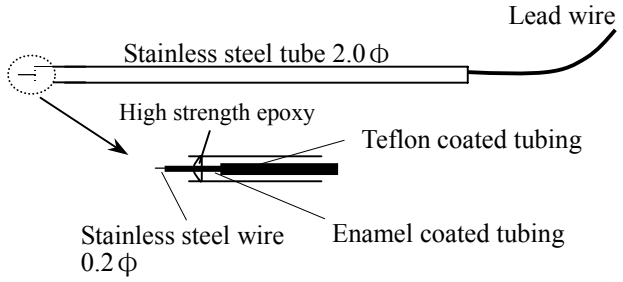

Fig. 2 A point-electrode resistivity probe

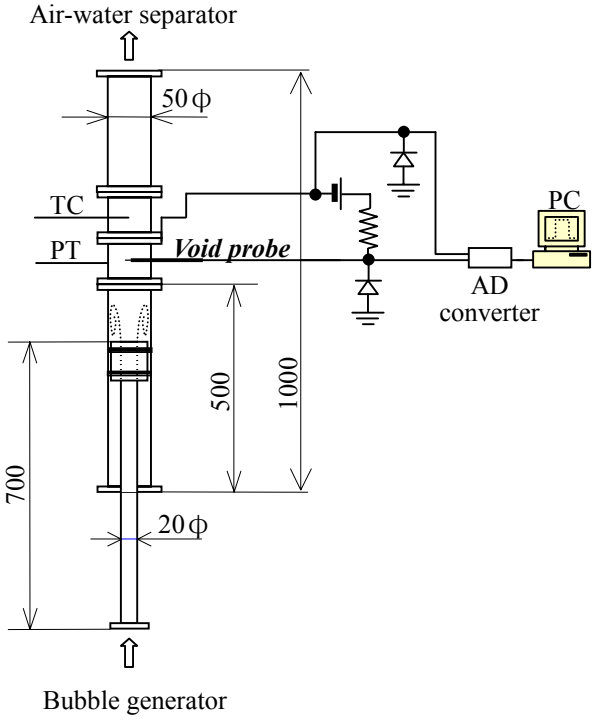

Fig. 3 Measuring section of void fraction

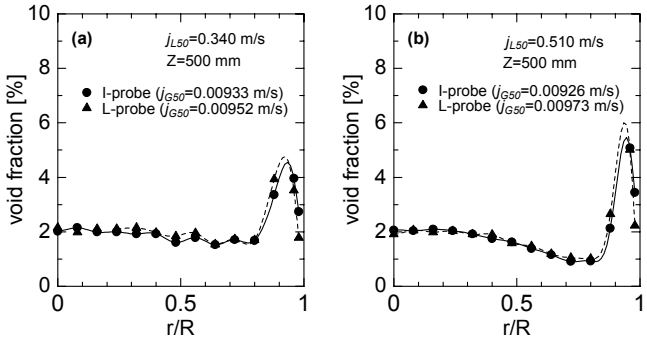

Fig. 4 Comparison measuring data between I-probe and L-probe

For more improve the precision, the liquid phase was kept as a constant electrolyte by potassium chloride, and it was monitored using an electrical conductivity meter. As for the void fraction measurement using a point-electrode resistivity probe, it is commonly measured by the upward type probe or L-type probe[10-12]. Before the void fraction measurement in the sudden expansion, we have compared with the values of void fraction between the I-type probe and the L-type beforehand. **Figure 4** shows the results of the void fraction distribution measured by both probes. It was not a serious problem in void fraction measurement. Therefore we preferably employed the I-type probe for measuring the radial void fraction accurately.

III. Analytical Models

1. Basic Equations

The basic equations used in the present numerical calculation of bubbly two-phase flow consist of Eulerian equations for continues liquid phase and Lagrangian equations for discrete bubbles. However, it is difficult for the sudden expansion channel geometry to accurately evaluate the liquid velocity distribution in the two-phase turbulent field. As the first step of the calculation, the Eulerian equations for liquid single-phase flow were employed as those for the two-phase flow. Commonly used mass and momentum conservation equations for continuous liquid phase were used; they are given by:

$$\frac{\partial \rho_L}{\partial t} = -(\nabla \cdot \rho_L \boldsymbol{u}_L) \tag{1}$$

$$\frac{\partial}{\partial t}\rho_L \boldsymbol{u}_L = -[\nabla \cdot \rho \boldsymbol{u}_L \boldsymbol{u}_L] - \nabla P - [\nabla \cdot \boldsymbol{\tau}] + \rho_L g \tag{2}$$

where t is the time, $\boldsymbol{u}$ the velocity, ρ the density, P the pressure, $\boldsymbol{\tau}$ stress tensor, g gravitational acceleration and the subscript L denotes the liquid phase.

The high-Reynolds number k-ε model for liquid single-phase flow was used as the turbulence model, proposed by Launder & Spalding[13]; they are given by:

$$\left(\frac{\partial}{\partial t}+\bar{u}_k\frac{\partial}{\partial x_k}\right)k$$
$$=\frac{1}{2}C_\mu\frac{k^2}{\varepsilon}\bar{e}_{ik}^{\,2}+\frac{\partial}{\partial x_k}\left\{\left(C_\mu\frac{k^2}{\varepsilon\sigma_k}+\nu\right)\frac{\partial k}{\partial x_k}\right\}-\varepsilon \tag{3}$$

$$\sigma_k=\frac{9C_\mu}{10C_T} \tag{4}$$

$$\left(\frac{\partial}{\partial t}+\bar{u}_k\frac{\partial}{\partial x_k}\right)\varepsilon$$
$$=\frac{1}{2}C_{\varepsilon1}C_\mu k\bar{e}_{ik}^{\,2}-C_{\varepsilon2}\frac{\varepsilon^2}{k}+\frac{\partial}{\partial x_k}\left\{\left(C_\mu\frac{k^2}{\varepsilon\sigma_\varepsilon}+\nu\right)\frac{\partial\varepsilon}{\partial x_k}\right\} \tag{5}$$

$$\sigma_k=\frac{3C_\mu}{2C_\varepsilon} \tag{6}$$

$$\mu_t=C_t\rho_L\frac{k^2}{\varepsilon} \tag{7}$$

where k denotes kinematic energy, ε kinematic energy dissipation rate, ν kinematic viscosity and μ_t turbulent viscosity of the liquid. Furthermore the value of constant σ_k is 1.0, σ_ε 1.3, C_1 1.44, C_2 1.92, C_3 0.0, C_t 0.09, respectively.

On the other hand, each bubble is treated as an individual particle on the Lagrangian coordinates. The conservation equations for discrete bubble are given by:

$$\frac{d}{dt}(\rho_b V_b)=0 \tag{8}$$

$$\rho_b\frac{d\boldsymbol{u}_b}{dt}=-\nabla\boldsymbol{P}-\boldsymbol{f}_i+\rho_b\boldsymbol{g} \tag{9}$$

where V denotes the volume and $\boldsymbol{f}_i$ the net interfacial force acting on the bubbles and the subscript b denotes the bubble. The pressure gradient $\nabla\boldsymbol{P}$ is given by the calculation results of pressure distribution data of liquid single-phase flow as well as liquid velocity.

Three-dimensional, one-way coupling calculation was performed using the Eq. (9) for tracking each bubble in the present study. It was assumed as a spherical bubble. From the bubble velocity $\boldsymbol{u}_b$ and the fluctuating velocity $\boldsymbol{u}_{turb}^b$, the position of each bubble $\boldsymbol{Z}_b$ is calculated by:

$$\frac{d\boldsymbol{Z}_b}{dt}=\boldsymbol{u}_b+\boldsymbol{u}_{turb}^b \tag{10}$$

2. Constitutive Equations

(1) Components of net interfacial force

For mathematically closing the basic equations, constitutive equations representing interfacial force acting on a bubble $\boldsymbol{f}_i$ is needed. Due to the complexity of the bubble motion in a turbulent flow field, no widely accepted model for $\boldsymbol{f}_i$ has been developed. Consequently it is said that reasonable evaluation of $\boldsymbol{f}_i$ is most essential. The $\boldsymbol{f}_i$ in the vertical pipe proposed by Okawa et al.[14, 15] is used for the sudden expansion channel. Hence, the net interfacial force acting on a bubble $\boldsymbol{f}_i$ is adequately expressed as the sum of the flowing four components in the present numerical calculation:

$$\boldsymbol{f}_i=\boldsymbol{f}_{sl}+\boldsymbol{f}_{wl}+\boldsymbol{f}_d+\boldsymbol{f}_{vm} \tag{11}$$

where $\boldsymbol{f}_{sl}$ denotes shear-induced lift force, $\boldsymbol{f}_{wl}$ wall-induced lift force, $\boldsymbol{f}_d$ interfacial drag force, and $\boldsymbol{f}_{vm}$ virtual mass force; the buoyant force is implicitly included in the momentum Eq. (9). Reliable correlations must be given for the components of $\boldsymbol{f}_i$. The correlations adopted for four components in Eq. (11) are described in the following sections.

(2) Correlations for the interfacial lateral forces

In the four components of $\boldsymbol{f}_i$, the forces mainly acting in the lateral direction are shear-induced lift force $\boldsymbol{f}_{sl}$ and the wall-induced lift force $\boldsymbol{f}_{wl}$. The $\boldsymbol{f}_{sl}$ is the force acting on a bubble in liquid shear field; the correlation for $\boldsymbol{f}_{sl}$ is given by Auton[16] and Drew and Lahey[17]:

$$\boldsymbol{f}_{sl}=C_{lift}\rho_L(\boldsymbol{u}_b-\boldsymbol{u}_L^b)\times(\nabla\times\boldsymbol{u}_L) \tag{12}$$

where $\boldsymbol{u}_L^b$ is the local liquid velocity evaluated at the bubble center position and C_{lift} the lift coefficient.

Since the drainage rate of liquid is restrained by the no-slip condition at the wall, bubble near the wall receives the wall lift force $\boldsymbol{f}_{wl}$ towards the center of channel; the following correlation developed by Antal et al.[18] is used for $\boldsymbol{f}_{wl}$:

$$\boldsymbol{f}_{wl}=\rho_L U_R^2\left[\frac{2}{d_b}C_{wl}+\frac{1}{y_b}C_{w2}\right]\boldsymbol{n}_w \tag{13}$$

where U_R denotes the relative velocity in the axial direction, d_b the sphere-equivalent bubble diameter, $\boldsymbol{n}_w$ the outward surface unit normal vector, C_{wl} = -0.06U_R-0.104 and C_{w2} = 0.147. Since the correlation is based on the pressure field around the bubble fixed in the uniform downward flow of liquid, there is uncertainly in the evaluation method of U_R if the velocity gradient around the bubble is very steep. For this reason, assuming that the wall lift force should be characterized by the relative velocity defined at the wall side of the bubble, the liquid velocity evaluated at the wall side of the bubble is used in the calculation of U_R. Therefore, the relative velocity between the bubble and liquid phase is used one of the important parameters in the correlations for the

lateral forces as indicated in Eqs. (12) and (13) in this calculation.

(3) Correlations for the drag force and virtual mass force

The interfacial drag force $\boldsymbol{f}_d$ is generally expressed by Ishii[19]:

$$\boldsymbol{f}_d = \frac{3}{4d_b} C_d \rho_L \left| \boldsymbol{u}_b - \boldsymbol{u}_L^b \right| (\boldsymbol{u}_b - \boldsymbol{u}_L^b) \tag{14}$$

where the drag coefficient C_d in the above equation is calculated by Fan and Tsuchiya[20]:

$$C_d = \frac{4g}{3U_b^2} d_b \tag{15}$$

where U_b is the terminal velocity. The U_b is estimated by the theoretical correlation proposed by Fan and Tsuchiya[20], in which U_b is the applicable to both the spherical and deformed bubble, the U_b is give by:

$$U_b = \left(U_{b1}^{-n} + U_{b2}^{-n} \right)^{\frac{-1}{n}} \tag{16}$$

where U_{b1} is the terminal velocity of spherical bubble, U_{b2} is the terminal velocity of deformed bubble, n is 1.6 and 0.8 for clean and contaminated systems.

The virtual mass force $\boldsymbol{f}_{vm}$ is calculated by the following widely used correlation. It is given by:

$$\boldsymbol{f}_{vm} = C_{vm} \rho_L \left(\frac{d\boldsymbol{u}_b}{dt} - \frac{d\boldsymbol{u}_L^b}{dt} \right) \tag{17}$$

where $\boldsymbol{u}_L^b$ is the local liquid velocity evaluated at the bubble center position and C_{vm} virtual mass coefficient. The C_{vm} is used as 0.5 proposed by Drew and Lahey[17].

(4) Models for fluctuating components in turbulent flow field

The bubble rise paths in turbulent flow field are usually unstable (Hinata et al.[21]). In the present models, the fluctuating velocity $\boldsymbol{u}_{\boldsymbol{turb}}^{\boldsymbol{b}}$ used for determining the bubble position in the turbulent flow field, as shown in Eq. (10). For evaluating the fluctuating component $\boldsymbol{u}_{\boldsymbol{turb}}^{\boldsymbol{b}}$, that is the origin of the rise path oscillation in the present models, it is assumed that the rise path oscillation is induced by the following three factors: (i) shear-induced turbulence in liquid phase; (ii) vortex shedding behind the bubble; and (iii) bubble wake formed behind the leading bubble. Consequently, $\boldsymbol{u}_{\boldsymbol{turb}}^{\boldsymbol{b}}$ is expressed as:

$$\boldsymbol{u}_{turb}^{b} = \boldsymbol{u}_{turb}^{si} + \boldsymbol{u}_{turb}^{vs} + \boldsymbol{u}_{turb}^{bw} \tag{18}$$

The amplitude of $\boldsymbol{u}_{turb}^{si}$ is supported to basically equal to the friction velocity $\boldsymbol{u}_f$, but the damping near the wall and the effect of eddy size relative to the bubble size are included:

$$\boldsymbol{u}_{turb}^{si} = \left\{ 1 - \exp\left(-\frac{y^+}{A^+} \right) \right\} u_f \times \min\left[1, \ \frac{l_e^{si}}{d_b} \right] \tag{19}$$

where y^+ and A^+ are the dimensionless distance from the wall and the empirical constant (the value of 16.0), respectively (Sato et el., 1981[22]). The size of the turbulent eddy l_e^{si} is estimated from the empirical correlation for mixing length developed by Nikuradse[23]:

$$y^+ = \frac{\boldsymbol{u}_f \, y_b}{\nu} \tag{20}$$

$$l_e^{si} = \left\{ 0.14 - 0.08 \left(1 - \frac{y_b}{R} \right)^2 - 0.06 \left(1 - \frac{y_b}{R} \right)^4 \right\} \times R \tag{21}$$

As often done in the Lagrangian simulation of droplet flow (Matsuura et al.[8]), the time period t_e^{si} is defined as the shorter time of the eddy life and bubble transit time.

$$t_e^{si} = \min\left(\frac{l_e^{si}}{\boldsymbol{u}_{turb}^{si}}, \frac{l_e^{si}}{\left| \boldsymbol{u}_b - \boldsymbol{u}_l^b \right|} \right) \tag{22}$$

The model of u_{turb}^{vs} is based on the experimental data on the oscillatory motion of single bubbles in stagnant liquid. From many experimental observations of bubble motion in stagnant liquid, ellipsoidal bubbles exhibit considerable oscillation whereas spherical bubbles and cap bubbles rise up almost rectilinearly. For the case of impure systems, Fan and Tsuchiya give the conditions for the oscillatory motion of bubbles[20]:

$$\mathrm{Re}_b > 202 = \mathrm{Re}_c \qquad E_o \le 40 \tag{23}$$

where Re_b, E_o are the bubble Reynolds number and Eötvös number. The u_{turb}^{vs} was evaluated by following correlation equation proposed by Okawa et al.[24] under the condition of Eq. (23).

$$u_{turb}^{vs} = 4 C_R u_r^{vs} \tag{24}$$

where the value of constant C_R is expressed by experimental results (Okawa et al.[24]). It is given as:

$$C_R = 0.1 \times \left[1 - \exp\left\{ -0.0061 \times (\mathrm{Re}_b - \mathrm{Re}_c) \right\} \right] \tag{25}$$

The time scale t_{turb}^{vs} is determined from the frequency of the rise path oscillation observed in a stagnant[20]:

$$t_e^{vs} = \frac{1}{2}\frac{d_b}{S_t u_r^{vs}} \tag{26}$$

where the Strouhal number S_t is given as the function of the bubble Reynolds number and the Morton number.

In bubbly two-phase flow, the bubble motion should be affected by the wake created by the leading bubbles. In this case, simple approach is adopted for evaluating the effects of leading bubbles. The wake velocity of the leading bubbles $\boldsymbol{u}_{turb}^{bw}$ is divided into the time-averaged component $\overline{\boldsymbol{u}}_{bw}$ and the fluctuating component $\boldsymbol{u}'_{bw}$. The vertical component of $\overline{\boldsymbol{u}}_{bw}$ is calculated by the correlation given by Stuhmiller et al.[25]:

$$\overline{u}_{bw}(x,r) = u_d(x)\exp\left(-\left[\frac{r}{r^*(x)}\right]^2\right) \tag{27}$$

where x and r are the axial and radial distances from the leading bubble, respectively; the modified correlations given by Trapp and Mortensen[26] are used for the spatial scale of the radial centerline wake velocity u_d. The amplitude of $\boldsymbol{u}'_{bw}$ is assumed to be proportional to $\overline{\boldsymbol{u}}_{bw}$:

$$\boldsymbol{u}'_{bw} = C_{bw}\overline{\boldsymbol{u}}_{bw} \tag{28}$$

where C_{bw} the constant value. The direction of $\boldsymbol{u}'_{bw}$ is also determined in a stochastic manner and its time scale t_{bw}^e is assumed to equal to that for the rise path oscillation given by Eq. (26).

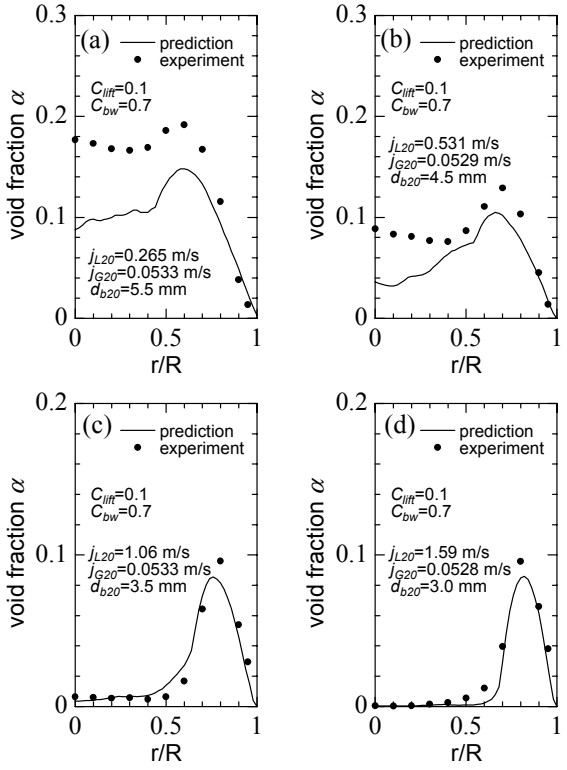

Fig. 5 Void fraction distribution in 20-mm tube

As for the present calculation, the interfacial forces acting on the bubbles are effective to predict the lateral void fraction distributions in bubbly two-phase flow in various liquid flow conditions. However, the bubble interaction is not considered to avoid the bubbles to overlap with other bubbles. Essentially, the bubble interaction models must be required for bubbly flow region. Besides, as the size of turbulent eddy is determined on the basis of the mixing length theory, the eddy size will be underestimated nearby the wall in a pipe. Additionally, it is not include quite important characteristic phenomena in the sudden expansion, such as high-shear layer, re-circulation flow, bubble breakup, bubble coalescence and bubble stagnation occurred by sudden expansion. Although these models should be further examined for a vertical pipe in two-phase turbulent flow, the calculation void fractions were predicted by considering the above-mentioned fluctuating velocity component. Therefore, in this calculation, the predicted bubble distributions were carried out for the relatively low liquid and gas volumetric velocity, that is, for low void fraction condition.

IV. Comparison of the results

1. Void fraction distributions in 20-mm tube

The first, the void fraction distributions in the 20-mm tube below the sudden expansion were confirmed. The void fractions were measured by using the void probe and its data processing system. Based on the trajectories of large number of single bubbles, the void fraction distributions were also predicted to compare with the measured void fraction data. **Figure 5** shows the experimental and numerical results performed in the 20-mm tube. The bubbles were introduced to be uniform from the bottom of the test channel, and the void fraction distributions were evaluated at 1.0 m downstream from the bottom. Where, the value of the lift coefficient C_{lift} in Eq. (12) was used as 0.1 proposed by Lahey and Drew[27, 28] in the turbulent two-phase flow field, and the constant value of the C_{bw} in Eq. (28) was adopted as 0.7. In **Fig. 5 (a)** and **(b)**, the discrepancy between the predictions and the experimental data appear near the center of the pipe. The forces mainly acting in the lateral direction are determined by the shear-induced lift force $\boldsymbol{f}_{sl}$ and the wall-induced lift force $\boldsymbol{f}_{wl}$ in this calculation. Since the shear-induced lift force acting in liquid shear field has a strongly effect on the migration to the wall in a pipe, bubbles traversed towards the wall due to liquid velocity as the bubble size decreases. In low liquid flux conditions, however, the $\boldsymbol{f}_{sl}$ is smaller and the bubble size is larger than that of the high liquid fluxes. As a result, the bubbles were situated near the center of the pipe. In this case, the relative velocity between liquid phase and bubble would be important factor for evaluating the void fraction distribution. However, it is said that the tendencies of the bubble distribution are basically captured in the calculation. While, in **Fig. 5 (c)** and **(d)**, the void fraction distributions appear

typical wall peak in the tube cross section. Under moderate liquid velocities, they were satisfactory expressed by the present model. The predictions of void fraction distributions were approximately agreed with experimental data in these flow conditions.

In the present calculation, the one-way simulation for bubble tracking is performed and the bubble interaction is not considered. Whereas, the calculation void fraction distributions in the 20-mm tube gave good agreements with experimental data reasonably well. Using the present models, the prediction of void fraction distribution is demonstrated for the sudden expansion channel.

2. Void fraction distributions in sudden expansion

(1) Effects of shear-induced lift force

In our previous study, the characteristic phenomena have been experimentally clarified in the sudden expansion. The flow patterns in the sudden expansion had the multi-dimensional structure that consists of (a) separation flow, (b) liquid share layer, (c) wall re-attachment point and (d) re-circulation flow (see **Fig. 6**). From the direct observation results, the bubble motion would be changed by the multi-dimensional flow patterns and structure depending on gas and liquid volumetric fluxes and bubble size[1]. Since the re-circulation region between the shear layer and reverse flow along the wall appears in the sudden expansion, we could observe the characteristic phenomena of bubbles at the just above the sudden expansion point, such as deformation, tear-off, breakup and coalescence of bubbles. Furthermore, it also revealed that bubbles did not migrate towards the wall in spite of the high shear layer existing; they are captured and tore off in the liquid shear layer region. However, such characteristic phenomena cannot be considered in this calculation. Therefore, using existing correlation equations for the shear-induced lift force tested the validity of the present calculation. The void fraction distributions were calculated using following lift coefficients.

Figure 7 shows the results of the effects of the lift force on the void fraction distribution. Bubble size was determined by changing the gas and liquid flow rates. The bubble distributions at the sudden expansion point were assumed to be uniform and the calculated void fraction of the tube cross-section in the sudden expansion were compared with various axial position of the sudden expansion. Horizontal-axis represents the radial position of the tube

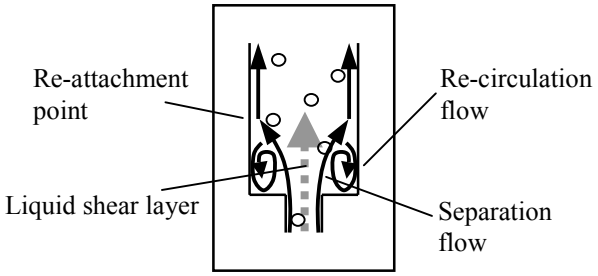

Fig. 6 Typical flow pattern in sudden expansion

cross-section in 50-mm tube, vertical axis means the local void fraction. Z is the axial position from the sudden expansion. Where "Z = 0" means the just sudden expansion point. In the case of C_{lift} = 0.0 in **Fig. 7** (a), bubbles were not diffused up to 100-mm axial position from the sudden expansion point. At the downstream of the sudden expansion, the bubble distribution gradually changed into core peak distribution due to non shear-induced lift force. On the other hand, the C_{lift} is estimated by the empirical correlation proposed by Tomiyama et al.[29], in which the influence of bubble deformation is considered and value of the C_{lift} turns positive to negative as the bubble size increases. According to the correlations, bubbles smaller than 5.6 mm tend to migrate towards the wall. As a result, the bubble distribution strongly appeared as wall peaking void fraction in the developing region of the sudden expansion, as shown in **Fig. 7** (c). Finally, in the case of C_{lift} = 0.1 in **Fig. 7** (b), proposed by Lahey and Drew for the two-phase turbulent flow[27), 28)], the bubbles were gradually diffused from the sudden expansion point to the downwards. After that, the void fraction distribution at the 500-mm axial position from the sudden expansion point gives rough agreement with the measured data. Through the comparison of these results, there are some problems of the lift coefficient for estimating the void fraction distribution in all cases. However, the value of 0.1 was adopted for C_{lift} in this time from these results.

(2) Effects of wake velocity of leading bubble

Since the bubble interaction is not basically considered in the present calculation, the calculation was tested by changing the only amplitude of the fluctuating component of leading bubble in Eq. (28). For verifying the bubble interaction for the void fraction distributions, the C_{bw} was

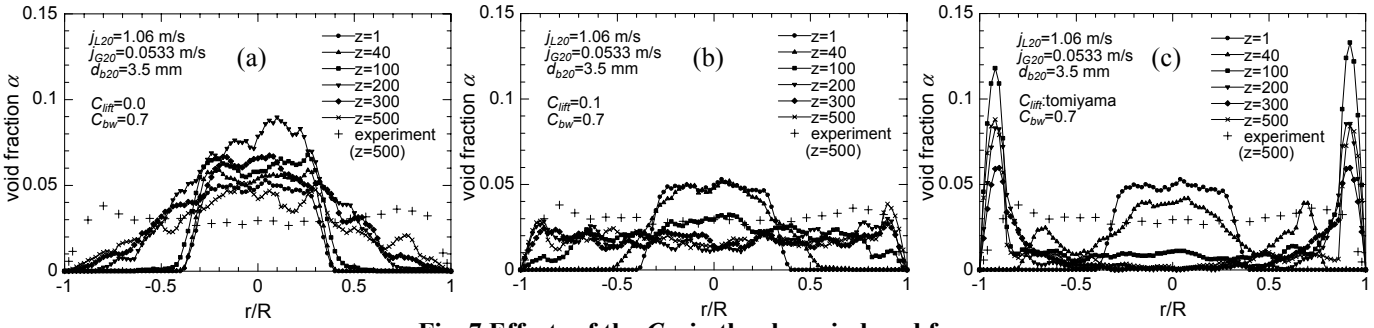

Fig. 7 Effects of the C_{lift} in the shear-induced force

parametrically changed. The results revealed that the effects of the C_{bw} on the void fraction distribution were not serious problems. There was slight difference for the forces acting in the lateral direction. Therefore, more detailed modeling for the bubble interaction such as bubble collision would be required to accurately evaluate for these cases. The value of 0.7 was adopted for the C_{bw} to estimate the void profiles in the sudden expansion as well as the case of 20-mm tube.

(3) Comparisons with experimental data measured in sudden expansion

The maximum void fractions in the 20-mm tube were measured near the wall in all flow conditions; especially the void peaks became prominent as the liquid velocity was increased up to 1.0 to 2.0 m/s. While it became obscure as the liquid velocity was further increased up to 3.0 to 5.0 m/s. These void fraction distributions become the initial conditions of the sudden expansion point. In this calculation, however, the bubble distributions at the sudden expansion point were assumed to be uniform in the 20-mm tube. **Figure 8** shows the examples of the calculated bubble distribution in the 50-mm tube. Approximately 20000 single-bubbles were treated in this calculation. The indicated marks and trajectories represent the center position of bubbles. In this case, though bubbles rose up laterally from the sudden expansion point towards the wall due to the shear lift force, they moved with swaying from the side to the center in the pipe. When the bubble size is smaller, the bubbles move towards the wall, while the number of bubbles

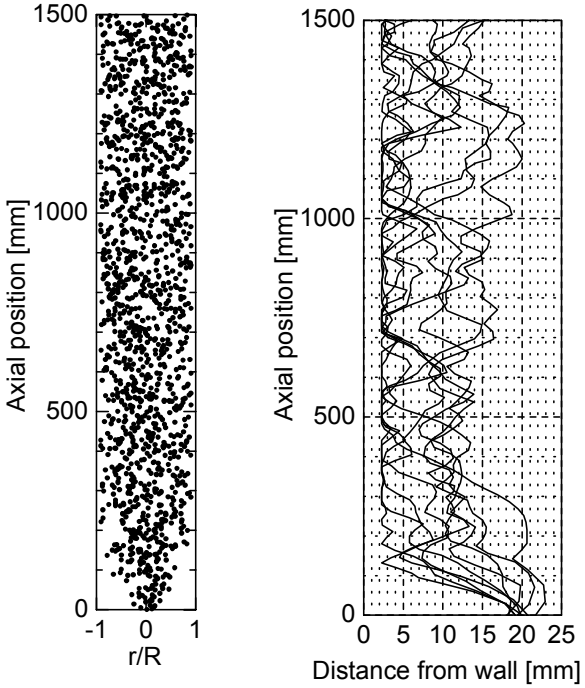

Fig. 8 Examples of single bubble distribution and Trajectories
(j_{L20}=0.531 m/s, j_{G20}=0.0533 m/s,d_{b20}=4.5mm)

in the core regions gradually increases with the increase of the bubble size.

The predicted and measured void fraction distributions in the 50-mm tube are shown in **Fig. 9**. For low liquid flux in **Fig. 9** (a), the bubble motions were roughly captured by the calculation from the sudden expansion point to the downstream. However, the value of the void fraction was underestimated for the measured data. In **Fig. 9** (b) and (c) for liquid velocity 0.5 to 1.0 m/s, the wall peak appeared in the developing region of the sudden expansion from the measured void data. It is due to the bubble stagnation near the wall at the downstream position from the sudden expansion point. As the influence of the bubble stagnation disappears at the downstream of the sudden expansion, the void fraction distribution became approximately uniform across the tube cross-section. These tendencies could not be fully predicted by this calculation. On the other hand, in **Fig. 9** (d) for 1.59 m/s**,** the liquid shear layer formed by sudden expansion was clearly appeared in 50-mm tube. As a result, bubbles were gradually diffused along the flow direction in the sudden expansion with re-circulating in the sudden expansion. In the experiment, they became the approximately uniform distribution at the 200-mm axial position from the sudden expansion point, after that the distribution appeared the wall-peak again. As for the calculation, however, the bubbles migrate towards the wall due to shear-induced lift force. Note that approximately 140-mm axial position from the sudden expansion means the re-attachment point of the single-phase flow calculated by standard k-ε model. Consequently, though the liquid shear layer is produced just above the sudden expansion point, the bubbles are not always affected by the velocity gradient due to the liquid shear layer in the developing region.

As mentioned above, the void peaking in the 20-mm tube appeared as the wall-peak in void fraction from the experimental results in all cases. As the two-phase flow develops along the flow direction, the wall peak distributions at the sudden expansion point are gradually disappeared. The distribution changes from the initial conditions of the 20-mm tube distribution to another distribution in the downstream of the sudden expansion point. The phase distribution would be affected not only by gas and liquid velocities but also by bubble size and configurations. However, the bubbles might be tore off and coalesced by the characteristic flow patterns in the developing region of the sudden expansion. Therefore, since the geometry of the sudden expansion affected the flow patterns and bubble size, the mechanisms of multi-dimensional phenomena become more complicated. As for the calculation results, the constitutive equations on the above-mentioned phenomena are not considered in the present models. Nevertheless, the bubble diffusions would be rough predicted by this calculation as a whole.

Although the predicted void fraction was underestimated in all cases, the bubble distribution in a pipe using three dimensional bubble tracking method was made a rough estimate by the present models. It pointed out that

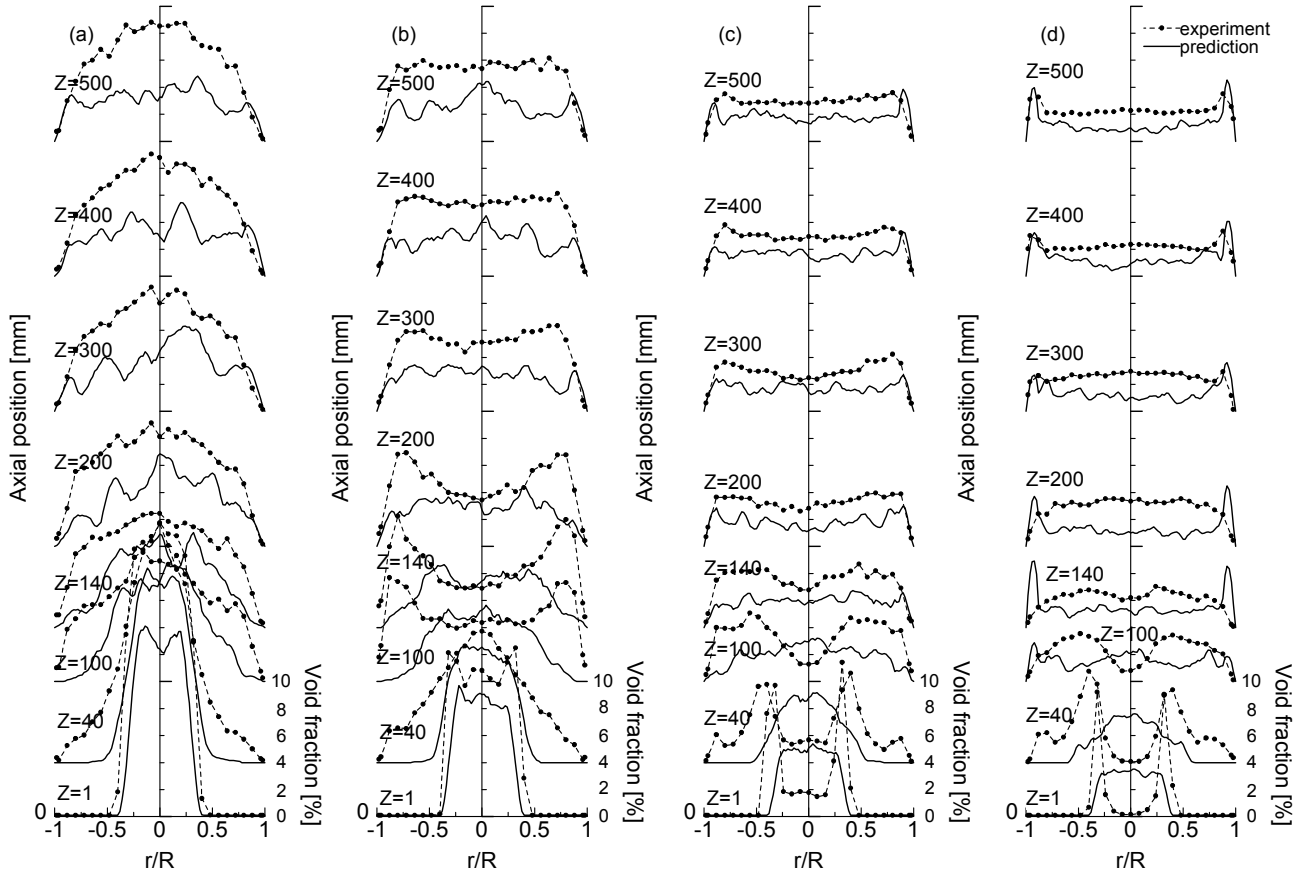

Fig. 9 Comparison of Predicted void fraction distributions with measured data (C_{lift}=0.1, C_{bw}=0.7)

the relative velocity between liquid phase and bubble might be not evaluated accurately in this flow condition, the shear-lift force and wall lift force should be reconsidered for such bubble size and liquid velocity, and bubble interaction should be considered in this calculation. Some factors migrating towards the center of a pipe might be acted on the bubbles. On the other hand, the coalescence and break up of bubbles in the high shear region are another important factors for the prediction. Therefore, to establish the numerical simulation models, which can predict accurately the multi-dimensional behavior of bubbly two-phase flow, more experimental information in multi-dimensional channel, detailed modeling such as the bubble interaction and two-phase turbulent model would be required.

V. Summery and Conclusions

Experimental and analytical studies were carried out on multi-dimensional behavior of upward gas-liquid two-phase flow in a vertical pipe with an axisymmetric sudden expansion, which is one of the typical multi-dimensional channel geometries. The first, the local void fractions in the tube cross sections were measured at several downstream positions of the sudden expansion using a point-electrode resistivity probe for various gas and liquid flow conditions. Next, the motion of single bubbles in the turbulent flow field in sudden expansion channel was calculated using a three dimensional one-way bubble tracking method, in which it takes into account shear-induced and wall-induced lift forces, drag force, virtual mass force, buoyancy and wall shear forces. Followings were noted through the experimental and numerical result.

1. The phase distributions in the sudden expansion showed that how the two-phase flow develops along the direction of the main flow. It also showed the distribution would be differed by changing the liquid and gas volumetric fluxes. The flow patterns and bubble size would be more complicated due to the characteristic phenomena occurred by sudden expansion.
2. The effects of bubble size, flow rates of gas and liquid phase, lift force acting on bubble etc. were evaluated. Although the void fraction is overestimated in all cases, the effect of liquid velocity on the void profile was made a rough estimate by the present model.
3. The lift force, bubble interaction and two-phase turbulence model were most important parameters in determining the void fraction distribution. In particular,

the models associated with the interaction between bubbles would be essential to predict the multi-dimensional behavior of two-phase flow.

Some detailed modeling would be carried out on the turbulence field near the expansion point. With use of appropriate modeling of turbulence parameters and lift force on the bubble, might predict multi-dimensional void fraction distribution agreed with the experimental data. Furthermore, the coalescence and break up of bubbles in the high shear region are another important factors in determining void fraction distribution as future studies.

References

1) Kondo, K. et al., "Flow patterns of gas-liquid two-phase flow in round tube with sudden expansion," *CD-ROM of Proc. 10th Int. Conf. on Nucl. Eng.,* ICONE10-22154, (2002).
2) Kondo, K. et al., "phase distribution of bubbly flow in round tube with sudden expansion," *Proc. Int. 3rd Korea-Japan Symposium on Nucl. Thermal Hydraulics and Safety*, 468, (2002).
3) Liels, D. R., Reed, W. H., "A semi-implicit method for two-phase fluid dynamics," *J. Computational Physics*, **26**, 390, (1978).
4) Anderson, J. G. M. et al, "BWR refill-reflood program task 4.7–TRAC," NUREG/CR-3623, EGG-2134, (1981).
5) Taylor, D. D. et al., "TRAC-BD1/MOD1: An advanced best estimate computer program for boiling water reactor transient analysis," NUREG/CR-3623, EGG-2294, (1984).
6) Kondo, K. et al., Applicability of two-fluid model and its constitutive equations to gas-liquid two-phase flow in sudden expansion, *CD-ROM of Proc. 11th Int. Conf. on Nucl. Eng.,* ICONE11-36187, (2003).
7) Tomiyama, A. et al., Bubble shape modelling for a 3D two-way bubble tracking method, *CD-ROM of Int. Conf. Multiphase Flow*, Lyon, France, Paper No.277, (1998).
8) Matsuura, K., Kataoka, I. and Serizawa, A., Droplet behavior analysis in annular-mist flow by two-way coupling method*, CD-ROM of Proc.7th International Conference on Nuclear Engineering*, Tokyo, Japan, ICONE7-7296, (1999).
9) Murai, Y., et al., "Numerical analysis of two-phase Convection around a cylinder in a Bubbly Flow," *Trans. Japan Soc. Mech. Eng.,* **60**-646, B, 1273, (2000).
10) Serizawa, A. and Kataoka, I., "Phase distribution in two-phase flow," 179, in: Transient Phenomena in Multiphase Flow, ed. by Afgan, N.H., (1988).
11) Liu, T. J., "Bubble size and entrance length effects on void development in a vertical channel," *Int. J. Multiphase Flow*, **19** (1), 99, (1993).
12) Zun, I., Kljenak, I. and Moze, S., "Space-time evolution of the nonhomogeneous bubble distribution in upward flow," *Int. J. Multiphase Flow*, **19** (1), 151, (1993).
13) Launder, B. E., and Spalding, D. B., "The numerical computation of turbulent flows," *Computer Methods in Appl. Mech. and Engng.* **3**, 269, (1974).
14) Okawa, T., Kataoka, I., Mori, M., Numerical simulation of single bubbles located in turbulent flow in vertical pipes using bubble tracking method, *Japanese J. Multiphase Flow*, **15** (2), 165, (2001).
15) Okawa, T., Kataoka, I., Mori, M., Numerical simulation of lateral phase distribution in turbulent upward bubbly two-phase flows, *Nuclear Engineering and Design*, **213**, 183, (2002).
16) Auton, T. R., The lift force on a spherical body in a rotational flow, *J. Fluid Mech*. **183**, pp.199-218, (1987).
17) Drew, D. A. and Lahey, R. T. Jr., The virtual mass and lift force on a sphere in rotating and straining inviscid flow, *Int. J. Multiphase Flow* **13** (1), 113, (1987).
18) Antal, S. P., Lahey, R. T. Jr. and Flaherty, J. E., Analysis of phase distribution in fully developed laminar bubbly two-phase flow, *Int. J. Multiphase Flow*, **17** (5), 635, (1991).
19) Ishii, M., Local drag laws in dispersed two-phase flow, NUREG/CR-1230, ANL-79-105, (1979).
20) Fan, L.-S. and Tsuchiya, K., Bubble wake dynamics in liquids and liquid-solid suspensions, Butterworth-Heinemann, Chap.2, (1990).
21) Hinata, S. et al., T., A study on bubble diffusion in two-phase flow, *Trans. JSME* **44**, 3526, (1978), [in Japanese].
22) Sato, Y., Sadatomi, M., Sekoguchi, K., Momentum and heat transfer in two-phase flow (I), *Int. J. Multipfase Flow*, **7**, 167, (1981).
23) Schlichting, H., Boundary layer theory, McGraw-Hill, Chap. 20, (1960).
24) Okawa, T. et al., Temperature effect on single bubble rise characteristics in stagnant distilled water, *Int. J. of Heat and Mass Transfer*, **46**, 903, (2003).
25) Stuhmiller, J. H., Ferquson, R. E., Meister, C. A., Numerical simulation of bubbly flow, EPRI NP-6557, (1989).
26) Trapp, J. A., Mortensen, G. A., A discrete particle model for bubble-slug two-phase flows, *J. Compt. Phys*., **107**, 367, (1993).
27) Lahey Jr., R. T., Lopez de Bertodano, M and Jones, Jr., O. C., Phase distribution in complex geometry conduits, *Nuclear Engineering and Design*, **141**, 177, (1993).
28) Lahey, R. T. Jr., Drew, D. A., The analysis of two-phase flow and heat transfer using a multidimensional, four field, two-fluid model, *Nuclear Engineering and Design*, **204**, 29, (2001).
29) Tomiyama, A. et al., Transverse migration of single bubbles in simple shear flows, *Chemical Engineering Science*, **57**, 1849, (2002).